

Engineering a Yellow Thermostable Fluorescent Protein by Rational Design

Matthew R. Anderson, Caitlin M. Padgett, Cammi J. Dargatz,^{||} Calysta R. Nichols,^{||} Keerti R. Vittalam, and Natasha M. DeVore*



Cite This: *ACS Omega* 2023, 8, 436–443



Read Online

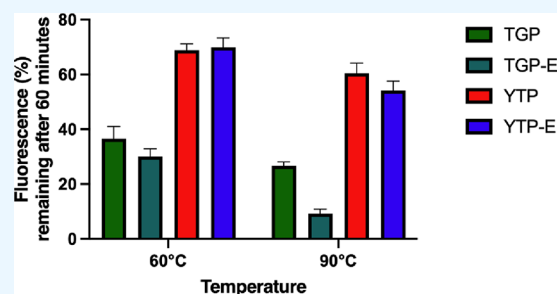
ACCESS |

Metrics & More

Article Recommendations

Supporting Information

ABSTRACT: Thermal green protein (TGP) is an extremely stable, highly soluble synthetic green fluorescent protein. The quantum yield of TGP is lower than the closest related natural fluorescent protein, monomeric Azami-Green. We improved the thermal recovery of TGP through the introduction of a chromophore mutation, Q66E. Furthermore, we developed a yellow thermal protein (YTP) via mutation of histidine 193 to tyrosine. Incorporation of Q66E into YTP (YTP-E) improved chemostability and pH stability. Both YTP and YTP-E have superior thermostability compared to TGP or TGP-E. These proteins offer a new option for green or yellow fluorescence under harsh chemical or thermal conditions.



INTRODUCTION

The discovery of green fluorescent protein (GFP) by Shimomura et al.¹ and further development through cloning, expression,² and engineering for desired colors and features has caused fluorescent proteins (FPs) to become an indispensable tool for multiple fields of research.^{3,4} The usefulness of FPs stem from the ability of the chromophore to form entirely from the protein sequence encoded by DNA spontaneously with only a requirement for molecular oxygen.³ The properties of GFP can be altered by mutation of specific protein residues, which result in changes in absorbance and fluorescence, faster protein folding, and other useful properties including biosensors and photo-switchable properties.^{5–8}

Thermo green protein (TGP) (RCSB PDB 4TZA) is an unusually thermostable and non-aggregation-prone fluorescent protein that was engineered from the fluorescent protein eCGP123.⁹ The fluorescent protein eCGP123 was derived from the synthetic consensus green protein (CGP) with directed evolution used to improve thermostability.^{9,10} TGP has strong advantages over other available FPs in experiments utilizing harsh thermophilic conditions or when there are concerns about protein aggregation affecting assay results, for example, in amyloid assays.^{6,11,12} TGP has also been used to construct a chimera between the light and heavy chain variable regions of antibodies, permitting one-step fluorescence assay for fluorescent-activated cell sorting.¹³ TGP has an 87% identity to monomeric Azami Green (mAG) from *Galaxea fascicularis* and 33.3% identity to the *Aequorea victoria* GFP. Like other fluorescent proteins, TGP is an 11-stranded β barrel protein with a central α helix that contains three residues (QGY) that form the chromophore.¹¹ This is the same QGY chromophore found naturally in mAG¹⁴ and the red

fluorescent protein DsRed,¹⁵ while in GFP, the chromophore is SGY.³ It is well established that alterations in the chromophore residues or local environment will have an impact on chromophore excitation and emission wavelengths. Blue, cyan, and yellow versions of GFP have been made by mutating residues in or around the chromophore.^{3,4,15} To generate a yellow version of GFP (YFP), histidine or tyrosine was incorporated under the chromophore, leading to a π -stack interaction.⁴ For YFP, additional rounds of mutation were required to improve the pH stability, folding rate, expression temperature, and sensitivity to chloride ions.^{16,17}

Our goal was to develop a yellow fluorescent version of TGP. In TGP, a π -stack interaction is already present with the chromophore and histidine 193. We used site-directed mutagenesis to mutate histidine 193 to tyrosine, leading to a yellow variant (YTP) that has better thermo and similar chemical and pH stability properties than TGP. However, this mutation results in a drastic loss in quantum yield. For both GFP and the monomeric derivative mRFP1 from DsRed, mutation at the first chromophore residue can alter their spectral characteristics. For GFP, one of the earliest improvements was made through mutation of serine 65 to threonine. This mutation improves ionization of the chromophore phenol, resulting in a single excitation peak at 489–490 nm.³ In DsRed, mutation of the glutamine at residue 66 can

Received: August 5, 2022

Accepted: November 29, 2022

Published: December 28, 2022

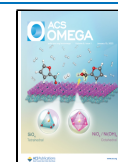


Table 1. Primers Used for Site-Directed Mutagenesis

mutation	forward primer	reverse primer
H193Y	CACGAGGTGGACTACCGCATTGAAATCCTG	CAGGATTTCAATGCGGTAGTCCACCTCGTG
Q6SE	CCAGCCTTCGAATACGGC	GCCGTATTCTGAAGGCTGG

	10	20	30	40	50	60	
TGP	MG	AHASVIKP	EMKIKLRMEG	AVNGHKFVIE	GEGIGKPYEG	TQTLDLTVEE	GAPLPFSYDI
TGP-E
YTP
YTP-E
		70	80	90	100	110	120
TGP	LTPAFQ	YGNR	AFTKYPEDIP	DYFKQAFPEG	YSWERSMTYE	DQGICIATSD	ITMEGDCFFY
TGP-E	E
YTP
YTP-E	E
		130	140	150	160	170	180
TGP	EIRFDGTNFP	PNGFVMQKKT	LKWEPESTEKM	YVEDGVLKGD	VEMALLEGG	GHYRCDFKTT	
TGP-E
YTP
YTP-E
		190	200	210	220	230	240
TGP	YKAKKDVRLP	DAHEVDHRIE	ILSHDKDYNK	VRLYEHAEAR	YSGGGSGGGA	SGKPIPNPLL	
TGP-E
YTP
YTP-E
		250					
TGP	GLDSTHHHHH	H					
TGP-E					
YTP					
YTP-E					

Figure 1. Protein sequence alignment of TGP-E, YTP, and YTP-E to TGP.

substantially change the excitation and emission spectra; subsequently, this led to the development of a series of yellow to red mFruit proteins.¹⁵ Altering the hydrogen bond network between the chromophore and fluorescent protein is known to affect the spectral properties and quantum yield of fluorescent proteins;¹⁸ accordingly, we mutated the chromophore residue glutamine 66 to glutamate in both the TGP and YTP proteins (TGP-E and YTP-E). We hypothesized that this change would not affect the volume of the amino acid, which may have caused steric clashes but may significantly alter the hydrogen bonding network between the chromophore and nearby residues. Although this single mutation did not significantly alter the quantum yield of TGP-E and YTP-E, it did change the thermal stability of these proteins. Both yellow variants had thermostability superior to that observed with either TGP or TGP-E. In addition, YTP-E is also more pH stable.

METHODS

Site-Directed Mutagenesis of TGP. The gene for TGP (synthetic protein) in the pETCK3 expression plasmid was provided from Los Alamos National Laboratory. Oligonucleotide primers (Table 1) were purchased from Thermo Fisher Scientific to incorporate a tyrosine at histidine 193 and a glutamate at glutamine 66. In addition, the Q66E mutation was made using TGP H193Y (YTP) to form a double mutant. The full sequence comparisons of TGP to mutant proteins are provided in Figure 1. Mutations were introduced using the Agilent QuickChange II site-directed mutagenesis kit. Plasmid purification was carried out using a GeneJET plasmid miniprep kit (Thermo Scientific). Purified plasmid was sequenced at ACGT, Inc. to verify proper incorporation of mutation.

Expression and Purification of Proteins. Proteins were expressed in *Escherichia coli* (*E. coli*) BL21(DE3) cells. A single colony was selected of each mutant and grown overnight in a 50 mL liquid Lennox broth (LB) with 50 μ g/mL kanamycin at 37 °C. Next, 25 mL of the overnight culture was added to 1 L of LB with 50 μ g/mL kanamycin and grown at 37 °C until the OD₆₀₀ was greater than 0.4. Then, 1 mM IPTG was added to induce protein expression and the temperature was reduced to 30 °C. Finally, *E. coli* cells were harvested by centrifugation after 1 day of growth and stored as pellets at -80 °C. In addition, for YTP and YTP-E, the volume of growth was doubled to 2 L in terrific broth media and growth after induction was increased to 3 days at a lower temperature of 26 °C.

Protein was extracted from *E. coli* cells using sonication on ice for a total of 90 s with 30 s rests in lysis buffer (0.1 M Tris, pH 7.4, 10% glycerol, 0.3 M NaCl) followed by centrifugation at 20,000 rpm. The lysate was then purified by affinity chromatography using NiNTA agarose (Gold Biotechnology). For YTP and YTP-E, the NiNTA affinity column was run by gravity. Protein was washed with 10 mM imidazole added to the lysis buffer and eluted in elution buffer (0.1 M Tris, pH 7.4, 10% glycerol, 0.2 M imidazole). Protein was further purified by ion exchange chromatography using a DEAE column (Bio-Rad) and eluted with a final buffer (0.1 M Tris, pH 7.4, 10% glycerol, 0.5 M NaCl). Purity was ascertained through SDS-PAGE using ImageJ (NIH) to quantify and determine the purity by densitometry of the 28 kDa band for each protein compared to other bands present in the gel (Supporting Information, Figure S1).¹⁹ For three preps of protein, the average purity \pm standard errors are TGP = 75 \pm 3%, TGP-E =

$92 \pm 8\%$, $YTP = 29 \pm 2\%$, and $YTP-E = 31 \pm 7\%$. Both yellow fluorescent proteins were never obtained at the same purity as TGP and TGP-E; however, under native gel conditions, the major lower-molecular-weight contaminant does not fluoresce (data not shown). Inclusion of ProBlock Gold Bacterial Protease Inhibitor Cocktail (GoldBio) at a 1× concentration prior to lysis during purification did not improve the protein purity, suggesting that this major lower-molecular-weight contaminant may result from improperly folded protein during the expression (Supporting Information, Figure S2). The protein was stored at $-80\text{ }^\circ\text{C}$ in the final buffer. Protein had no difference in absorbance or fluorescence after 6 months of storage or repeated freeze–thaws (up to three times). The protein can be concentrated up to 200 mg/mL with no aggregation noted. Protein was thawed from the freezer prior to use in experiments.

Measurement of Ultraviolet (UV) and Visible Absorption Spectra. Absorbance spectra of variant TGP proteins were measured using purified proteins with a Shimadzu UV-2101PC spectrophotometer from 700 to 250 nm. Extinction coefficients at 280 nm were determined using ProtParam at Expasy.org.²⁰ Extinction coefficients for chromophores were determined at absorbance below 0.2 (I_{\max}^{Abs}) and computed using Beer's law. These measurements represent the calculation from the protein with the greatest purity from at least three purifications.

Measurement of Fluorescence Excitation and Emission Spectra and Quantum Yield. Fluorescence emission and excitation spectra were recorded on a Perkin Elmer LS55 fluorescence spectrometer with a 1 cm pathlength quartz cuvette at room temperature. To determine the quantum yield, the relative method was used with fluorescein (Fisher Scientific, Acros Chemicals, 99% pure laser grade) in 0.1 M NaOH as a standard, $\phi_F = 0.792$. Equation 1 below was used to determine the quantum yield values of each protein^{21–23}

$$\phi_X = \phi_{ST} \left(\frac{m_X}{m_{ST}} \right) \left(\frac{n_{ST}^2}{n_X^2} \right) \quad (1)$$

where the subscripts ST and X denote the standard and sample, respectively, ϕ is the fluorescence quantum yield, m is the slope of the line obtained by the plot of integrated fluorescence intensity (peak area) vs absorbance, and n is the refractive index of the solvent wherein the literature value is 1.33 for solvents used.²¹ A total of five or six measurements were taken for each sample at different concentrations. The standard error was calculated based on the linear regression fit, and error propagation was used to determine the error associated with each quantum yield measurement. A one-way analysis of variance (ANOVA) was used to compare the statistical significance of the QY of YTP, YTP-E, TGP, and TGP-E. Total absorbance values below 0.1 were used for all measurements. The accuracy was cross verified using harmine, $\phi_F = 0.45$, as a positive control. The value derived for harmine (Fisher Scientific, Indofine Chemical, 99% purity) with eq 1 was within 5% of the literature value.

Thermostability Measurements. Thermostability measurements for TGP, TGP-E, YTP, and YTP-E were acquired on an RT-PCR (QuantStudio 6 Applied Biosystems). For measurements, 3.75 pmol of the sample was added to assay buffer (0.1 M Tris, pH 7.4, 20 mM MgCl_2) in a 96-well PCR plate. For stability measurements, fluorescence was recorded at $25\text{ }^\circ\text{C}$ prior to temperature ramping to either 90 or $60\text{ }^\circ\text{C}$ after

which fluorescence was measured once per minute. An FAM filter was used, which has $470 \pm 15\text{ nm}$ excitation and $520 \pm 15\text{ nm}$ emission. For analysis, the percent fluorescence remaining was normalized to the fluorescent value at $25\text{ }^\circ\text{C}$ prior to heating. For unfolding and refolding kinetics, the same sample set-up was used with the temperature ramped from 25 to $99\text{ }^\circ\text{C}$ at a rate of $0.9\text{ }^\circ\text{C}$ per minute and recorded every 1.7 s. The temperature was then rapidly decreased to $25\text{ }^\circ\text{C}$, and the fluorescence was measured every 30 s for an hour. The temperature ramping followed by recovery (one cycle) was repeated consecutively four times (four cycles) with at least four biological replicate samples.

Chemical Denaturation. Purified fluorescent protein (3.75 pmol) was diluted into an assay buffer (0.1 M Tris, pH 7.4, 20 mM MgCl_2) containing guanidinium HCl (Gdn HCl) concentrations ranging from 0 to 8 M. Fluorescence was measured on a SpectraMax M5 plate reader. The excitation and emission wavelengths were set to excitation at 485 nm, emission at 508 nm for TGP and TGP-E and to excitation at 510 nm, and emission at 525 nm for YTP and YTP-E. To determine the time required to reach equilibrium, measurements of samples in 0–8 M Gdn HCl were obtained after 1 h, 5 days, and 10 days at room temperature. The 5- and 10-day measurements were consistent for all proteins, indicating that equilibrium was reached. Fluorescence was normalized to the value of the 0 M guanidinium HCl sample for analysis and to ensure that measurements were at equilibrium, the 10-day incubation time was used. The C_m of Gdn HCl (where a 50% loss in fluorescence/melting occurred) were determined from sigmoidal dose–response fitting using GraphPad Prism 9. All experiments were done with four biological replicates (from two preparations of protein), and standard error (SEM) is shown as error bars.

Sensitivity to pH. Purified fluorescent protein was diluted 15-fold into 0.1 M glycine-phosphate-citrate buffers with 0.1 M NaCl at varying pH levels (3–10) and incubated at room temperature for 1 h. Fluorescence was measured with the SpectraMax M5 plate reader with the same excitation and emission wavelengths as the chemical denaturation assay. Fluorescence was normalized to the pH with the highest fluorescence for each protein.⁵ In the case of YTP-E, each trial had a different pH value that was maximal; therefore, when plotted in replicate, there was no single pH with a consistent value near 100%. All experiments were performed with five biological replicates from two preparations of proteins.

RESULTS

TGP Mutants. With pETCK3 TGP as an initial material, histidine 193 was mutated by site-directed mutagenesis to tyrosine resulting in a redshifted protein (YTP). An additional mutation in the chromophore, Q66E, was incorporated into both TGP and YTP (TGP-E and YTP-E). Incorporation of desired mutation was verified by DNA sequencing at ACGT, Inc.

Properties of Fluorescent Proteins. All four proteins were expressed in BL21(DE3) cells and purified. After purification, their excitation and emission properties (Figure 2 and Table 1) were obtained. The spectral features of YTP were similar to other yellow fluorescent proteins with an excitation wavelength of 513 nm and an emission wavelength of 526 nm. TGP-E is slightly redshifted compared to TGP. The quantum yields were significantly decreased for YTP and YTP-E compared to TGP (Table 2).¹¹ Our quantum yield

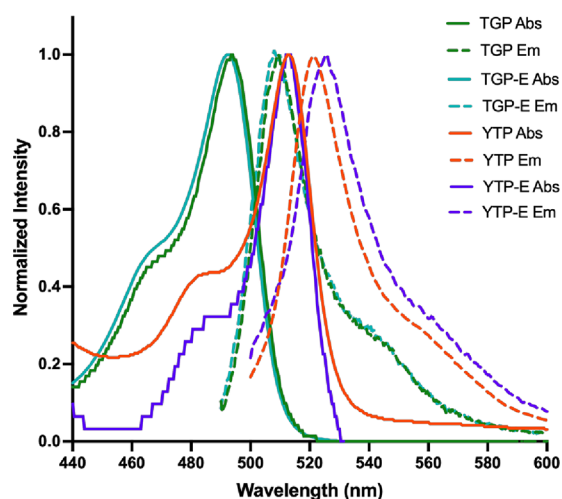


Figure 2. Absorbance and emission spectra overlay for TGP, TGP-E, YTP, and YTP-E; the intensity is normalized to maximal chromophore absorption or emission.

Table 2. Spectroscopic Properties of TGP, TGP-E, YTP, and YTP-E^a

protein	excitation λ_{\max} (nm)	emission λ_{\max} (nm)	ϵ ($M^{-1} \text{ cm}^{-1}$)	ϕ_F
TGP	493 ^b	507 ^b	64,000 ^b	0.83 ± 0.04 ^a
TGP-E	493	509	48,000	0.84 ± 0.04 ^a
YTP	395, 513	522	3400	0.02 ± 0.0007 ^a
YTP-E	513	526	3400	0.03 ± 0.001 ^a

^aA one-way ANOVA was performed to compare the quantum yield of TGP, TGP-E, YTP, and YTP-E. There was a statistically significant difference between TGP and YTP or YTP-E ($p < 0.0001$) and between TGP-E and YTP or YTP-E ($p < 0.0001$). There is no statistical difference between the ϕ_F of TGP and TGP-E ($p = 0.9516$) and YTP and YTP-E ($p = 0.9236$). ^bAs reported in Close et al.¹¹

measurements had a higher value of 0.83 ± 0.04 for TGP and than the value reported by Close et al. of $\phi_F = 0.66$.¹¹ The Q66E mutation did not affect the quantum yield of either TGP-E or YTP-E compared to TGP or YTP, respectively.

The pH stability of each of these proteins was compared by observing changes in fluorescence with pH. Most of the mutants had similar pH sensitivities to TGP, with pK_a values of 6.7 for TGP (95% confidence interval, 6.5–6.9), 6.7 for YTP (95% confidence interval, 6.5–7.0), and 6.6 for TGP-E (95% confidence interval, 6.4–6.9) (Figure 3A). YTP-E appears to lack sensitivity to pH and as such, its plot appears invariant with pH (Figure 3B). TGP appears to be sensitive to greater pH values as at pH 10, it only had $49 \pm 5\%$ of fluorescence, so these pH values were not included in Figure 3A for TGP.

The unfolding kinetics and thermostability at high temperatures of TGP, TGP-E, YTP, and YTP-E were investigated using a RT-PCR instrument with an FAM filter set at 470 ± 15 nm excitation and 520 ± 15 nm emission. For all RT-PCR-based experiments, 3.75 pmol of the respective protein was used and diluted into the assay buffer, and fluorescence was monitored in real time. For the unfolding experiment, the temperature was ramped from 25 to 99 °C slowly and then rapidly cooled back to 25 °C and held there for an hour to monitor refolding and repeated three times for a total of four cycles (Figure 4). For clarity, each cycle is plotted on the same plot for each protein to demonstrate the protein's ability to

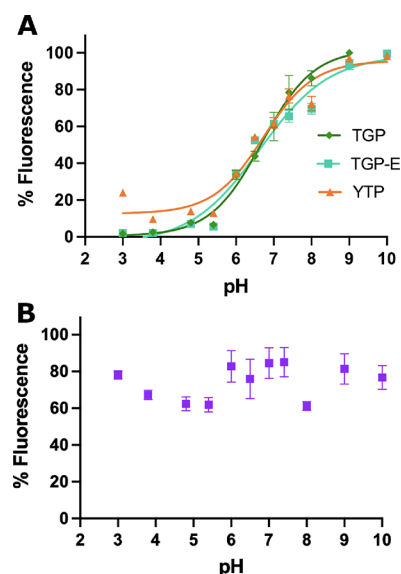


Figure 3. (A) pH titration of TGP ($R^2 = 0.95$), TGP-E ($R^2 = 0.96$), and YTP ($R^2 = 0.92$). Fluorescent intensities were measured after 1 h of incubation at buffers at 3–10 pH. The excitation and emission wavelengths were set to 485 nm excitation and 508 nm emission for TGP and TGP-E and 510 nm excitation and 525 nm emission for YTP. (B) pH titration of YTP-E. A 510 nm excitation and 525 nm emission wavelength were used. For all proteins, experiments were performed with five trials and data is normalized to the highest fluorescence in each trial regardless of pH. Error bars represent the standard error of the mean.

recover with each progressive cycle of heating. An elongated plot with each cycle shown linearly is available in the Supporting Information (Figure S3). The stability of both YTP and YTP-E is evident in their return to pre-heat fluorescence levels with each cycle (Figure 4B,D). Neither YTP nor YTP-E completely lost their fluorescence at 99 °C. YTP maintains 33% of its fluorescence in the first cycle at 99 °C and 45% of fluorescence in cycles two, three, and four (Figure 4B). YTP also has levels of fluorescence that are higher than initially recorded after the first and second cycle of heating. YTP-E maintains 40% of fluorescence at 99 °C and recovers close to 100% of fluorescence after each heating step (Figure 4D). Both TGP and TGP-E have diminishing levels of fluorescence with progressive cycles and only have 1–5% of fluorescence remaining at 99 °C (Figure 4A,C). Thirty percent of initial fluorescence is recovered for TGP at return to 25 °C in the first cycle, 18% after the second heating cycle, 12% after the third cycle, and only 9% after four cycles of heating (Figure 4A). TGP-E follows this same trend but has better recovery levels (Figure 4C). After the first cycle of heating, when returned to 25 °C, TGP-E recovers 48% of fluorescence, 34% after the second heating cycle, 28% after the third heating cycle, and 24% after the fourth cycle. We cannot report T_m values as this phenomenon is likely due to a combination of protein unfolding (likely for TGP and TGP-E) and loss of fluorescence due to vibrational disruptions in the local chromophore environment as the proteins are heated.¹⁰ This theory is supported by the very fast recovery in fluorescence when the temperature is cooled to 25 from 99 °C.

The thermostability of TGP, TGP-E, YTP, and YTP-E was also measured with temperatures held at 60 and 90 °C for an hour (Figure 5). Data is normalized to fluorescence at 25 °C before samples were heated. Once again, a drop in fluorescence

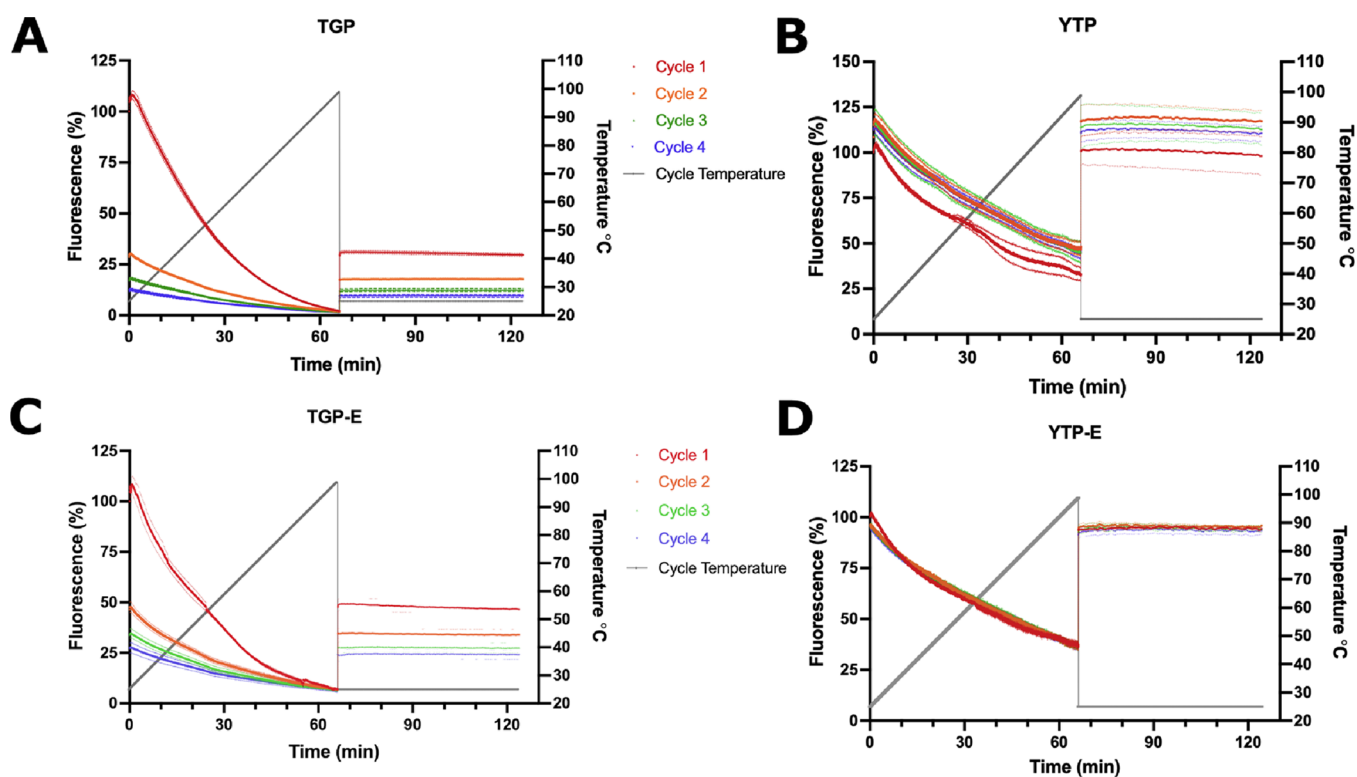


Figure 4. (A) TGP, (B) YTP, (C) TGP-E, and (D) YTP-E were assayed for thermostability using a real-time PCR machine. Four consecutive cycles of heating from 25 to 99 °C followed by a rapid cooling to 25 °C for an hour were obtained. For clarity, each cycle is shown as a separate color on the same plot. The x axis of all plots represents the time each cycle was carried out. The gray line on each graph represents the temperature at each time with the right y axis. Fluorescence is normalized to the % fluorescence at 25 °C before heating began in cycle 1. Error bars represent standard error of the mean and are shown as dashed lines of the same color above and below each cycle's mean plot.

occurs quickly upon heating, but then equilibrium is reached. Both YTP and YTP-E are remarkably stable with only a 60% loss in initial fluorescence upon heating and a small increase in fluorescence occurring though the 1 h duration of the experiment at 60 °C. TGP and TGP-E are similar at 60 °C, but at 90 °C, TGP-E is less stable with only 10% of its fluorescence remaining after 1 h versus the 30% remaining for TGP. It is notable that TGP-E displays a loss in fluorescence during the first 20 min of the 90 °C incubation; this does not occur for any of the other proteins.

Protein stability was further characterized by equilibrium unfolding with increasing concentrations of Gdn HCl (Figure 6A). The C_m was 6.0 M Gdn HCl for TGP (95% CI of 5.6–6.2), 5.0 M Gdn HCl for TGP-E (95% CI of 4.7–5.4), and 4.2 M Gdn HCl for YTP (95% CI of 4.0–4.3). Complete loss in fluorescence was not observed for TGP-E at 8 M Gdn HCl. YTP-E showed no specific trend in unfolding with increasing Gdn HCl with about 20% loss in fluorescence overall regardless of concentration (Figure 6B).

DISCUSSION

A yellow version of TGP was made using site-directed mutagenesis to incorporate H193Y, a single essential mutation below the chromophore; this resulted in a shift of the excitation wavelength to 513 nm and emission wavelengths to 525 nm. Tyrosine was previously shown to shift GFP toward yellow at the corresponding location.^{17,24} For both TGP and YTP, the chromophore glutamine 66 was mutated to a glutamate in order to alter the hydrogen bonding network near the chromophore. Based on the known crystal structure of

TGP (PDB 4TZA), there is no basic amino acid located near the mutated glutamate, so a salt bridge cannot explain this effect. In the crystal structure of TGP, the glutamine located at position 66 in TGP hydrogen bonds to glutamine 42 and the main chain of leucine 211. Glutamine 42 could still maintain a hydrogen bond with the mutated glutamate 66. All mutations were sequence verified, expressed in *E. coli* BL21(DE3) cells, purified by affinity and ion exchange chromatography, and then characterized. Notably, the glutamate does not substantially alter chemical equilibrium or pH stability for TGP-E. There are some differences between the thermostability of TGP-E and TGP. TGP-E has better recovery after multiple heat cycles (Figure 4C) but loses some fluorescence when heated at 90 °C (Figure 5B). These experiments are looking at thermostability in two different ways: TGP-E has better recovery after exposure to high temperatures, while TGP maintains its fluorescence for longer durations when heated.

TGP was originally designed to be extremely stable and aggregation resistant; similarly, these derivative proteins maintain these same properties.¹¹ Superfolder green fluorescent protein, which was specifically engineered to fold at an enhanced rate, was also further engineered to withstand thermophilic conditions and has been successfully used in thermophilic bacteria as a location tag.^{6,25,26} A similar real-time PCR-based thermal stability assay was completed with sfGFP and sfGFP(N39D/A179A), and total loss of fluorescence was observed for both proteins by 95 °C.²⁶ The same research group also developed an sfYFP(N39D/A179A) protein that had significantly higher thermal stability than the green proteins; however, it also rapidly lost all fluorescence above

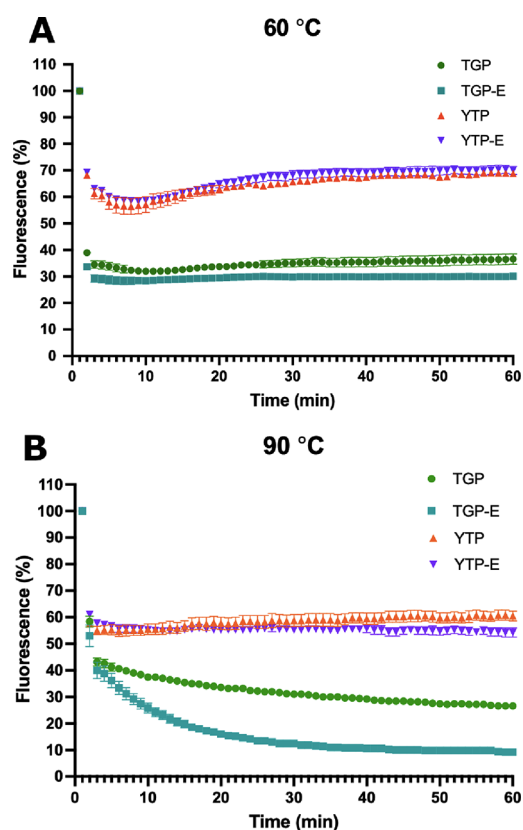


Figure 5. (A) Thermostability of TGP, TGP-E, YTP, and YTP-E at 60 °C. (B) Thermostability of TGP, TGP-E, YTP, and YTP-E at 90 °C. Error bars represent the standard error of the mean.

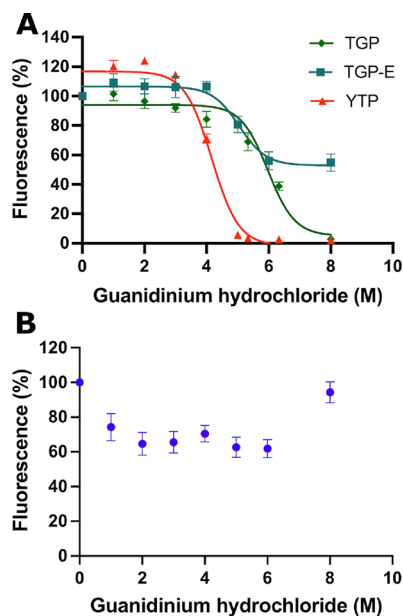


Figure 6. (A) Equilibrium unfolding plots for TGP ($R^2 = 0.92$), TGP-E ($R^2 = 0.74$), and YTP ($R^2 = 0.98$) with increasing concentrations of guanidine hydrochloride after 10 days. (B) Equilibrium unfolding plot of YTP-E with increasing concentrations of guanidine hydrochloride after 10 days. Percent fluorescence was normalized based on the fluorescence of samples with no guanidine hydrochloride added. Error bars represent the standard error of the mean.

95 °C.²⁶ Fast-folder thermostable yellow fluorescent protein (FFTS-YFP) was developed specifically for thermostability.

Although the researchers did not perform an equivalent thermal melting experiment with FFTS-YFP, an experiment with a steady temperature of 90 °C with a real-time PCR instrument was reported with a 50% loss in fluorescence at 10.6 min.⁵ YTP and YTP-E are both about 10% above this level in fluorescence at the same time point. Both YTP and YTP-E had significantly lower losses in fluorescence with heating and increased stability over time compared to TGP and TGP-E. They both recover fluorescence at or above baseline levels with four rounds of heating (Figure 4B,D). YTP has an increase in fluorescence after heating to 99 °C. We hypothesize that this may be due to a gain in correctly folded YTP molecules after heating. In addition, a notable increase in both chemical equilibrium and pH stability occurs with the Q66E single mutation of YTP-E compared to YTP.

A shortcoming of both YTP and YTP-E is the low quantum yield. The low quantum yields are likely due to disruption of a prominent hydrogen bond network located beneath the chromophore.^{14,27} In TGP, the histidine at 193 participates in a π -stack with the tyrosine of the chromophore. It was noted that mutation of residue 193 from histidine to glutamine substantially decreased the quantum yield to 0.003 in photo-switchable chromoprotein Phanta, which was derived from eCGP123.^{27,28} TGP is also derived from eCGP123 but lacks the photo-switchable ability yet maintains high quantum yield fluorescence. Additional mutations at the same site in Phanta were tried, and similar drops in quantum yields were observed for those mutants as well, ascribed to disruption of both the hydrogen bond network and the π -stacking interaction with the chromophore histidine.²⁷ With YTP and YTP-E, the loss in quantum yield is more likely due to hydrogen bond disruption alone as the π -stacking interaction should be conserved between the tyrosine and chromophore. Much like TGP, but unlike Phanta, the yellow variants reported in this paper are not able to photo-switch (data not shown).¹¹ Further mutations will be required to restore this hydrogen bond network and increase the quantum yield in YTP-E. A combination of rational and directed evolution may be used to further improve the YTP-E protein in the future.

In conclusion, we have introduced one additional mutation, Q66E, into TGP to produce TGP-E, a green thermal protein with increased chemical stability and improved cycling thermostability. We also developed a yellow thermal protein based on TGP both with and without the Q66E mutation. Both yellow thermal proteins are remarkably thermally stable. The YTP-E construct also has good pH and chemical stability. YTP-E would make an excellent choice for experiments requiring lower pH, for example, experiments in acidic organelles such as the lysosomes or increased temperature found in thermophilic organisms.

■ ASSOCIATED CONTENT

Supporting Information

The Supporting Information is available free of charge at <https://pubs.acs.org/doi/10.1021/acsomega.2c05005>.

(Figure S1) SDS-page of TGP, TGP-E, YTP, and YTP-E after two column purification; (Figure S2) SDS-page of YTP and YTP-E with and without protease inhibitor included during purification; (Figure S3) progressive four cycles of heating and recovery for TGP, TGP-E, YTP, and YTP-E (this is the same data as shown in Figure 4, only plotted as continuous cycles) (PDF)

Accession Codes

TGP: RCSB PDB 4TZA

AUTHOR INFORMATION**Corresponding Author**

Natasha M. DeVore – Department of Chemistry and Biochemistry, Missouri State University, Springfield, Missouri 65897, United States;  orcid.org/0000-0003-0772-8929; Email: ndevores@missouristate.edu

Authors

Matthew R. Anderson – Department of Chemistry and Biochemistry, Missouri State University, Springfield, Missouri 65897, United States

Caitlin M. Padgett – Department of Chemistry and Biochemistry, Missouri State University, Springfield, Missouri 65897, United States

Cammi J. Dargatz – Department of Chemistry and Biochemistry, Missouri State University, Springfield, Missouri 65897, United States; Present Address: Missouri State Highway Patrol Crime Lab, 425 E Phelps St., Springfield, Missouri 65806, United States (C.J.D)

Calysta R. Nichols – Department of Chemistry and Biochemistry, Missouri State University, Springfield, Missouri 65897, United States

Keerti R. Vittalam – Department of Chemistry and Biochemistry, Missouri State University, Springfield, Missouri 65897, United States; Greenwood Laboratory School, Springfield, Missouri 65897, United States

Complete contact information is available at:

<https://pubs.acs.org/10.1021/acsomega.2c05005>

Author Contributions

^{||}C.J.D. and C.R.N. contributed equally. M.R.A. completed all thermostability and TGP-E and YTP-E experiments. C.M.P. completed all quantum yield measurements. C.J.D. and C.R.N. both completed experiments with TGP and YTP. K.R.V. was involved in purifying YTP. The manuscript was written, and experiments were designed by N.M.D. All authors have given approval to the final version of the manuscript.

Funding

This project was funded by a Missouri State University Internal Faculty Research Grant.

Notes

The authors declare no competing financial interest.

ACKNOWLEDGMENTS

The *E. coli* plasmid pETCK3 TGP was obtained from Los Alamos National Lab through a Material Transfer Agreement. We would also like to thank the Missouri State University Department of Biology for use of their QuantStudio 6 Applied Biosystems RT-PCR instrument.

ABBREVIATIONS

FP, fluorescent protein; TGP, thermal green protein; TGP-E, thermal green protein Q66E; YTP, yellow thermal protein; YTP-E, thermal yellow protein Q66E; GFP, green fluorescent protein; Gdn HCl, guanidine hydrochloride

REFERENCES

(1) Shimomura, O.; Johnson, F. H.; Saiga, Y. Extraction, Purification and Properties of Aequorea, a Bioluminescent Protein from the

Luminous Hydromedusan, Aequorea. *J. Cell. Comp. Physiol.* **1962**, *59*, 223–239.

(2) Chalfie, M.; Tu, Y.; Euskirchen, G.; Ward, W. W.; Prasher, D. C. Green Fluorescent Protein as a Marker for Gene Expression. *Science* **1994**, *263*, 802–805.

(3) Tsien, R. Y. The Green Fluorescent Protein. *Annu. Rev. Biochem.* **1998**, *67*, 509–544.

(4) Ormö, M.; Cubitt, A. B.; Kallio, K.; Gross, L. A.; Tsien, R. Y.; Remington, S. J. Crystal Structure of the Aequorea Victoria Green Fluorescent Protein. *Science* **1996**, *273*, 1392–1395.

(5) Aliye, N.; Fabbretti, A.; Lupidi, G.; Tsekos, T.; Spurio, R. Engineering Color Variants of Green Fluorescent Protein (GFP) for Thermostability, pH-Sensitivity, and Improved Folding Kinetics. *Appl. Microbiol. Biotechnol.* **2015**, *99*, 1205–1216.

(6) Cava, F.; de Pedro, M. A.; Blas-Galindo, E.; Waldo, G. S.; Westblade, L. F.; Berenguer, J. Expression and Use of Superfolder Green Fluorescent Protein at High Temperatures in Vivo: A Tool to Study Extreme Thermophile Biology. *Environ. Microbiol.* **2008**, *10*, 605–613.

(7) Holder, A. N.; Ellis, A. L.; Zou, J.; Chen, N.; Yang, J. J. Facilitating Chromophore Formation of Engineered Ca²⁺ Binding Green Fluorescent Proteins. *Arch. Biochem. Biophys.* **2009**, *486*, 27–34.

(8) Habuchi, S.; Ando, R.; Dedeker, P.; Verheijen, W.; Mizuno, H.; Miyawaki, A.; Hofkens, J. Reversible Single-Molecule Photoswitching in the GFP-like Fluorescent Protein Dronpa. *Proc. Natl. Acad. Sci. U. S. A.* **2005**, *102*, 9511–9516.

(9) Dai, M.; Fisher, H. E.; Temirov, J.; Kiss, C.; Phipps, M. E.; Pavlik, P.; Werner, J. H.; Bradbury, A. R. M. The Creation of a Novel Fluorescent Protein by Guided Consensus Engineering. *Protein Eng., Des. Sel.* **2007**, *20*, 69–79.

(10) Kiss, C.; Temirov, J.; Chasteen, L.; Waldo, G. S.; Bradbury, A. R. M. Directed Evolution of an Extremely Stable Fluorescent Protein. *Protein Eng., Des. Sel.* **2009**, *22*, 313–323.

(11) Close, D. W.; Paul, C. D.; Langan, P. S.; Wilce, M. C. J.; Traore, D. A. K.; Halfmann, R.; Rocha, R. C.; Waldo, G. S.; Payne, R. J.; Rucker, J. B.; Prescott, M.; Bradbury, A. R. M. Thermal Green Protein, an Extremely Stable, Nonaggregating Fluorescent Protein Created by Structure-Guided Surface Engineering. *Proteins* **2015**, *83*, 1225–1237.

(12) Cai, H.; Yao, H.; Li, T.; Hutter, C. A. J.; Li, Y.; Tang, Y.; Seeger, M. A.; Li, D. An Improved Fluorescent Tag and Its Nanobodies for Membrane Protein Expression, Stability Assay, and Purification. *Commun. Biol.* **2020**, *3*, 753.

(13) Velappan, N.; Close, D.; Hung, L.-W.; Naranjo, L.; Hemez, C.; DeVore, N.; McCullough, D. K.; Lillo, A. M.; Waldo, G. S.; Bradbury, A. R. M. Construction, Characterization and Crystal Structure of a Fluorescent Single-Chain Fv Chimera. *Protein Eng., Des. Sel.* **2021**, *34*, gzaa029.

(14) Ebisawa, T.; Yamamura, A.; Kameda, Y.; Hayakawa, K.; Nagata, K.; Tanokura, M. The Structure of MAG, a Monomeric Mutant of the Green Fluorescent Protein Azami-Green, Reveals the Structural Basis of Its Stable Green Emission. *Acta Crystallogr., Sect. F: Struct. Biol. Cryst. Commun.* **2010**, *66*, 485–489.

(15) Shaner, N. C.; Campbell, R. E.; Steinbach, P. A.; Giepmans, B. N. G.; Palmer, A. E.; Tsien, R. Y. Improved Monomeric Red, Orange and Yellow Fluorescent Proteins Derived from *Discosoma* Sp. Red Fluorescent Protein. *Nat. Biotechnol.* **2004**, *22*, 1567–1572.

(16) Griesbeck, O.; Baird, G. S.; Campbell, R. E.; Zacharias, D. A.; Tsien, R. Y. Reducing the Environmental Sensitivity of Yellow Fluorescent Protein: Mechanism and Applications. *J. Biol. Chem.* **2001**, *276*, 29188–29194.

(17) Nagai, T.; Ibata, K.; Park, E. S.; Kubota, M.; Mikoshiba, K.; Miyawaki, A. A Variant of Yellow Fluorescent Protein with Fast and Efficient Maturation for Cell-Biological Applications. *Nat. Biotechnol.* **2002**, *20*, 87–90.

(18) Khrameeva, E. E.; Drutsa, V. L.; Vrzheschch, E. P.; Dmitrienko, D. V.; Vrzheschch, P. V. Mutants of Monomeric Red Fluorescent Protein MRFP1 at Residue 66: Structure Modeling by Molecular

Dynamics and Search for Correlations with Spectral Properties. *Biochemistry (Moscow)* **2008**, *73*, 1085–1095.

(19) Alonso Villela, S. M.; Kraïem, H.; Bouhaouala-Zahar, B.; Bideaux, C.; Aceves Lara, C. A.; Fillaudeau, L. A Protocol for Recombinant Protein Quantification by Densitometry. *MicrobiologyOpen* **2020**, *9*, 1175.

(20) ExPASy - ProtParam tool; <https://web.expasy.org/protparam/> (accessed 2022-05-27).

(21) Lawson-Wood, K.; Upstone, S. L.; Evans, K. Determination of Relative Fluorescence Quantum Yields using the FL 6500 Fluorescence Spectrometer (014216_01); <https://www.semanticscholar.org/paper/Determination-of-Relative-Fluorescence-Quantum-the-Lawson-Wood-Upstone/98aa2345147db6757c06a1324133e5e0773e1a1f> (accessed 2022-06-06).

(22) Recording Fluorescence Quantum Yields; <https://www.horiba.com/int/applications/materials/material-research/quantum-dots/recording-fluorescence-quantum-yields/> (accessed 2022-01-18).

(23) Würth, C.; Grabolle, M.; Pauli, J.; Spieles, M.; Resch-Genger, U. Relative and Absolute Determination of Fluorescence Quantum Yields of Transparent Samples. *Nat. Protoc.* **2013**, *8*, 1535–1550.

(24) Wachter, R. M.; Elsliger, M.-A.; Kallio, K.; Hanson, G. T.; Remington, S. J. Structural Basis of Spectral Shifts in the Yellow-Emission Variants of Green Fluorescent Protein. *Structure* **1998**, *6*, 1267–1277.

(25) Pédelacq, J.-D.; Cabantous, S.; Tran, T.; Terwilliger, T. C.; Waldo, G. S. Engineering and Characterization of a Superfolder Green Fluorescent Protein. *Nat. Biotechnol.* **2006**, *24*, 79–88.

(26) Frenzel, E.; Legebeke, J.; van Stralen, A.; van Kranenburg, R.; Kuipers, O. P. In Vivo Selection of SfGFP Variants with Improved and Reliable Functionality in Industrially Important Thermophilic Bacteria. *Biotechnol. Biofuels* **2018**, *11*, 8.

(27) Don Paul, C.; Traore, D. A. K.; Olsen, S.; Devenish, R. J.; Close, D. W.; Bell, T. D. M.; Bradbury, A.; Wilce, M. C. J.; Prescott, M. X-Ray Crystal Structure and Properties of Phanta, a Weakly Fluorescent Photochromic GFP-Like Protein. *PLoS One* **2015**, *10*, No. e0123338.

(28) Don Paul, C.; Kiss, C.; Traore, D. A. K.; Gong, L.; Wilce, M. C. J.; Devenish, R. J.; Bradbury, A.; Prescott, M. Phanta: A Non-Fluorescent Photochromic Acceptor for PcFRET. *PLoS One* **2013**, *8*, No. e75835.